INTERNATIONAL JOURNAL FOR NUMERICAL AND ANALYTICAL METHODS IN GEOMECHANICS, VOL. 20, 785–814 (1996)

THE EFFECTIVE STRESS PRINCIPLE: INCREMENTAL OR FINITE FORM?

BERNHARD A. SCHREFLER

Istituto di Scienza e Tecnica delle Costruzioni, Universita' di Padova, Via Marzolo 9, I-35131 Padova, Italy

AND

DARIUSZ GAWIN

Department of Building Physics and Building Materials, Technical University of Lodz, Al. Politechniki 6, 93-590 Lodz, Poland

Dedicated to Erwin Stein in occasion of his 65th birthday

SUMMARY

Different expressions of the effective stress principle can be found in the literature, in particular some are written in finite form and others in incremental form. For the purpose of the paper we take for granted that stress–strain relationships exist or can be obtained for the effective stress coming from both formulations. We investigate the consequences of the choice of particular finite or differential forms when they are introduced in a weak form of the linear momentum balance equation of two- of three-phase porous media for its numerical solution. For partially saturated geomaterials the importance of the capillary pressure–saturation relationship is pointed out.

KEY WORD: effective stress principle; stress–strain relationships; porous media

1. INTRODUCTION

The effective stress usually is defined as the stress which controls stress–strain, volume change and strength behaviour in a porous medium, independent of the magnitude of the pore pressure.[1, 2] Its introduction goes back to Terzaghi[3] and Fillunger,[4] and proved to be extremely successful in soil mechanics. There are however many formulations for this principle, as shown in Reference 2. For the stress–strain behaviour of fully saturated geomaterials, the most common expression is

$$\sigma' = \sigma + \alpha \mathbf{I}\, p_\ell \tag{1}$$

where σ' is the effective stress, σ the total stress tensor, $\mathbf{I}$ the unit second-order tensor, p_ℓ the pore water pressure and, for isotropic material,

$$\alpha = 1 - \frac{K_T}{K_S}, \tag{2}$$

usually called Biot's constant, with K_T the bulk modulus of the solid skeleton and K_S the bulk modulus of the grains. In fact, as shown in Reference 2 this expression was derived by Biot,[5] Gassman,[6] Biot and Willis,[7] Geertsma,[8] Skempton,[1] Serafim,[10] Nur and Byerlee[11] and Bishop.[12] This expression is in finite form. The stresses are traction-positive and pore pressure, compression positive.

In Reference, 2 Lade and de Boer derived a new form, involving four parameters. This formulation based on principles of mechanics is valid for all types of materials. A distinction is

CCC 0363–9061/96/110785–30

Received 22 November 1995
Revised 22 February 1996

made between compressibilities of grains and skeleton, due to total stress and pore pressures. Two distinct expressions are then obtained for effective stress in granular material and in solid rock with interconnected pores, respectively. The expression for solid rock with interconnected pores is similar to equation (1), but in incremental form. From experiments, Lade and de Boer conclude that Terzaghi's proposed effective stress principle works well for stress magnitudes encountered in most geotechnical applications, but significant deviations occur at very high stresses.

For $\alpha = 1$, as may be assumed for soils,[1] and is assumed here, the incremental form is an exact differential and in initial-boundary value problems, as specified in Section 3, both the integral and differential form may be used, as long as the initial conditions are specified accordingly. This can be immediately checked by integrating the incremental form with respect to time which is a dummy variable.

The problem with partially saturated soils is different. A commonly used form of the effective stress principle for partially saturated soils was first developed by Bishop[13] and may be written as

$$\sigma' = \sigma + \mathbf{I}[p_g - \chi(p_g - p_l)], \tag{3}$$

where p_g is the gas pressure and χ the Bishop parameter, usually a function of the degree of saturation. All pressures here are relative pressures, usually measured with respect to the atmospherical pressure. The same expression, but with Bishop's parameter equal to the water degree of saturation was obtained by Lewis and Schrefler[14] using volume averaging. Further it was obtained by Hassanizadeh and Gray[15] using averaging techniques and the entropy inequality and including interfacial phenomena. The procedure proposed by Coleman and Noll[16] was used in that instance.

Based on the effective stress obtained from equation (3), constitutive laws for silt and for silty sands have been derived in Reference 17 with $\chi = S(2 - S)$, for clay in Reference 18 and 19 with $\chi = S$, and in Reference 20 for sand, again with $\chi = S$. Shear strength of unsaturated soils has further been modelled in Reference 21 using the effective stress in the form of equation (3) (with $p_g = p_{atm}$) and the capillary pressure–saturation relationship. All these models have been validated with respect to experiments.

An expression similar to equation (3), but in incremental form was obtained by Coussy[22] using the Clausius–Duhem inequality and macroscopic variables. The free volume energy of the open system is a function of strain, mass and temperature. In this case the incremental form is not an exact differential and its integral differs from the form of equation (3), as will be shown in the next section. But then Gudehus[23] argues that thermodynamical aspects in porous media are far from being clarified. In fact, the grain skeleton with repulsive contact forces is not in thermodynamic equilibrium. The contact region is not rate independent and slow diffusion of imperfections in the bulk and along the solid–solid interface is always present.

There is obviously no consensus about which form of the effective stress principle to adopt. We take here for granted that appropriate constitutive relationships, describing the stress–strain behaviour, can be established based on the effective stress coming from one or the other formulation. They have been derived as shown above, at least for the effective stress which stems from the finite form of the effective stress principle. The form of this principle is of importance when it is introduced in the linear momentum balance (equilibrium) equation of a three-phase geomaterial: the resulting linear balance equations are different. This is true even for linear elastic soil behaviour which is here adopted to eliminate the influence of non-linearities coming from the stress–strain relationship. Further we assume here the simplest case of equation (3) or the incremental form, with $\chi = S$. It will be shown that the capillary pressure–saturation relationship (retention curve) plays a fundamental role. First the importance of this relationship

in the difference between the two formulations of the effective stress principle is investigated, using three different retention curves and assuming a decrease of saturation. The corresponding diagrams say however not much about the influence on realistic laboratory or field situations. We investigate hence on two initial-boundary value problems what differences arise when applying the effective stress principle in incremental form or in finite one. The first problem is about desaturation of an initially fully saturated soil sample and the second one is about non-isothermal consolidation of partially saturated soil sample, including phase change. The solution of the coupled system of equations, formed by the mass balance equations for the fluids and the equilibrium equation (and energy balance equation) for the multiphase system gives the fluid pressures and saturation (and temperature) history needed for our purpose and simultaneously the displacement field which is the most effected one by the choice of the form of the effective stress principle.

It is reminded that many numerical solutions of consolidation, e.g. References 24 and 25, soil dynamics problems in fully and partially saturated conditions[26–28] and thermo-hydro-mechanical problems[29] use the effective stress principle in finite form.

2. THE EFFECTIVE STRESS PRINCIPLE INVESTIGATED

As already mentioned in the previous section, for the case with both air and water flowing in the pores of a partially saturated porous medium there are in literature different formulations of an effective stress relationship. The first one was derived by Bishop[13] and by Bishop and Blight,[30] when puting the Bishop parameter $\chi = S$, and has the following finite form:

$$\sigma' = \sigma + p\,\mathbf{I} \tag{4}$$

where p is the average pressure of fluids surrounding the grains (called also pressure in the solid phase), which equals to

$$p = S p_\ell + (1 - S)p_g - p_{atm} = p_g - S p_c - p_{atm}. \tag{5}$$

In the latter expression $p_c = p_g - p_\ell$ is the capillary pressure and S the water degree of saturation. The atmospheric pressure term in equation (5) has been added because we use here absolute pressures, whereas in equation (3) relative ones have been applied.

Often the pressure term in equation (4) is multiplied by α, the Biot's constant, given by equation (2), to account for the volumetric deformability of the particles. In References 1, 7 and 26, α was shown to be less or equal to one.

Equation (4) is often used in its incremental or time differentiated form, e.g. Reference 31. The latter can be expressed as

$$\dot{\sigma}' = \dot{\sigma} + (\dot{p}_g - \dot{S} p_c - S\dot{p}_c)\mathbf{I} \tag{6}$$

On the other hand, a similar expression as equation (4), but in incremental form, was obtained by Coussy,[22]

$$\mathrm{d}\sigma' = \mathrm{d}\sigma + (\mathrm{d}p_g - S\,\mathrm{d}p_c)\mathbf{I} \tag{7a}$$

It can also be rewritten in the adequate time differentiated form:

$$\dot{\sigma}' = \dot{\sigma} + (\dot{p}_g - S\dot{p}_c)\mathbf{I} \tag{7b}$$

It can be seen immediately that (6) differs from (7b), that (7a) is not an exact differential and (4) cannot be obtained from (7a) by simple integration. In fact, by integrating (7a) by parts, with

adequate change of integration limits we obtain

$$\sigma' = \sigma + \left(p_g - p_{atm} - \int_0^{p_c^*} S(p_c)\,dp_c\right)\mathbf{I} \tag{8a}$$

$$= \sigma + \left(p_g - p_{atm} - S\,p_c - \int_{S^*}^{1} p_c(S)\,dS\right)\mathbf{I} \tag{8b}$$

where the term p_{atm} has been added as a constant of integration, while p_c^* and S^* are specified values of capillary pressure and saturation, respectively.

The difference is given by

$$\int_{S^*}^{1} p_c(S)\,dS. \tag{9}$$

Its geometrical interpretation is explained in Figure 1, where the area corresponding to this integral has been dashed. From Figure 1 it results evidently that this term is of importance for materials, whose saturation decreases considerably already for relatively low capillary pressure values, e.g. for sands.

To estimate the possible influence of this term, the capillary pressure–saturation relationships of three different sands (Figure 2) have been applied. The first is that of the Del Monte sand, measured by Liakopoulos (in the range of saturation from 1 to about 0·9) (Reference 32). The second one was given by Safai and Pinder[33] and the last one by Brooks and Corey.[34] In all these relationships hysteresis is neglected. Figure 3(a) shows the resulting values of the integral (9) for the three analysed sands, Figure 3(b) presents the comparison of the pressures in the solid phase calculated by means of the formulae (5) and (8), while Figure 3(c) depicts their ratio, assuming that the gas pressure equals the atmospheric pressure value.

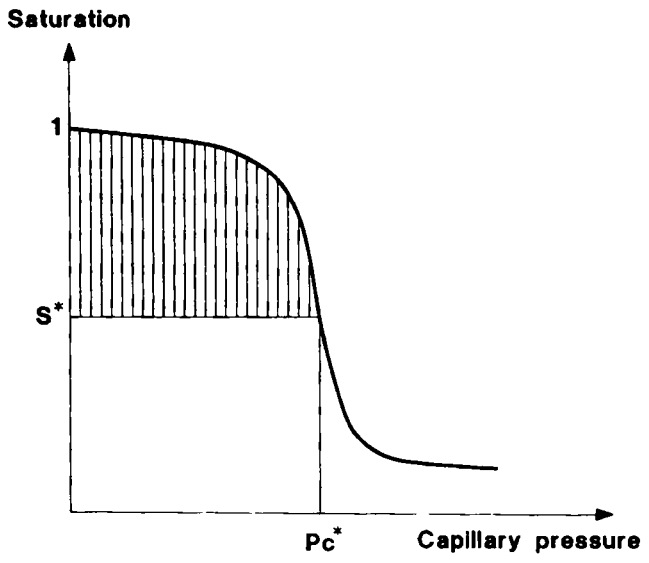

Figure 1. Geometrical interpretation of the integral term (9)

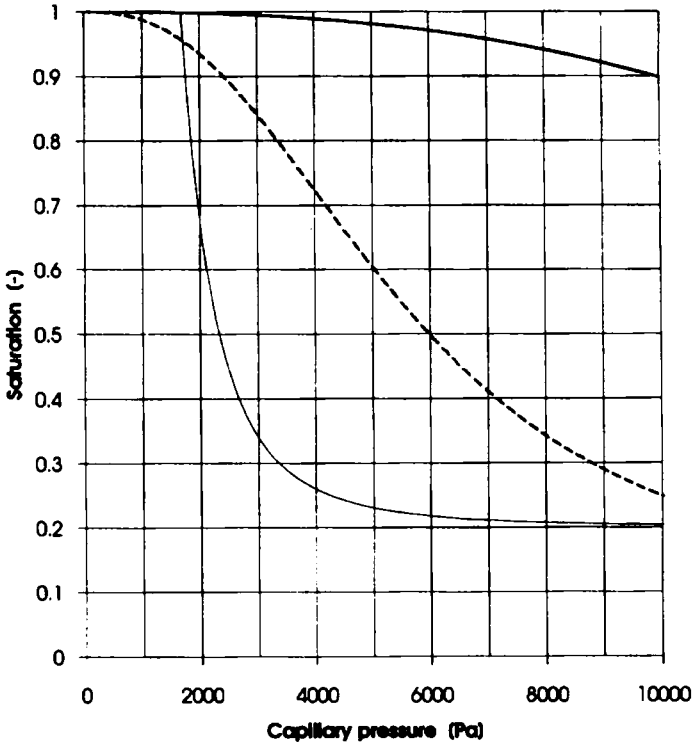

Figure 2. Capillary pressure – saturation diagram for three different sands: according to Liakopoulos[32] (solid line), Safai and Pinder[33] (broken line), Brooks and Corey[34] (fine line)

Further conclusion can be drawn by comparison of equations (6) and (7b). They show that the difference between them depends upon the time rate of desaturation process, as well as on the capillary pressure value. The difference between Bishop's and Coussy's formulations of the effective stress will hence be the most evident for a fast desaturation process of a relatively coarse grain material, e.g. sand, being in funicular saturation state[35] (high water relative permeability value), close to the saturation range, where a rapid fall of capillary pressure curve occurs. Varying degree of saturation implies flow of the interstitial fluids, hence to analyse the effect of the above-mentioned differences initial-boundary value problems have been chosen. The flow is considered here induced by mechanical or thermomechanical action.

The examples of Section 4, appropriately chosen, will show that this difference is negligible, at least at high saturation values, where in usual soil mechanics problems the pressures have a non-negligible influence on the solid skeleton behaviour, i.e. where the problem is still coupled.

3. AN INITIAL-BOUNDARY VALUE PROBLEM AND ITS NUMERICAL SOLUTION

All the computations presented in this paper have been performed by means of the mathematical and numerical model proposed in References 29, 36 and 37. Below only the final form of the governing equations and some informations about numerical solution are briefly summarized.

The model consists of four balance equations: mass of the dry air, mass of the water species (both liquid water and vapour, phase change is taken into account), enthalpy of the whole medium

(latent heat of the phase change is considered) and linear momentum of the multiphase medium. They are completed with an appropriate set of constitutive and state equations, as well as some thermodymanic relationships. The governing equations of the model, expressed in terms of the chosen state variables: gas pressure p_g, capillary pressure p_c, temperature T and displacement vector $\mathbf{u}$, are as follows (all the symbols are explained in Appendix):

Dry air conservation equation:

$$\phi \frac{\partial}{\partial t}[(1-S)\rho_{ga}] + \alpha(1-S)\rho_{ga}\frac{\partial}{\partial t}(\nabla\cdot\mathbf{u}) + \nabla\cdot(\rho_{ga}\,\mathbf{v}_g) - \nabla\cdot(\rho_g\,\mathbf{v}_{gw}^{d}) = 0 \tag{10}$$

water species (liquid–vapour) conservation equation:

$$\begin{aligned}\phi \frac{\partial}{\partial t}\Big[(1-S\rho_{ga}] + \alpha(1-S)\rho_{ga}\frac{\partial}{\partial t}(\nabla\cdot\mathbf{u}) + \nabla\cdot(\rho_{ga}\,\mathbf{v}_g) + \nabla\cdot(\rho_g\,\mathbf{v}_{gw}^{d})\\ = -\phi\rho_l\frac{\partial S}{\partial t} - \alpha S\rho_l\frac{\partial}{\partial t}(\nabla\cdot\mathbf{u}) - \nabla\cdot(\rho_l\,\mathbf{v}_l)\Big]\end{aligned} \tag{11}$$

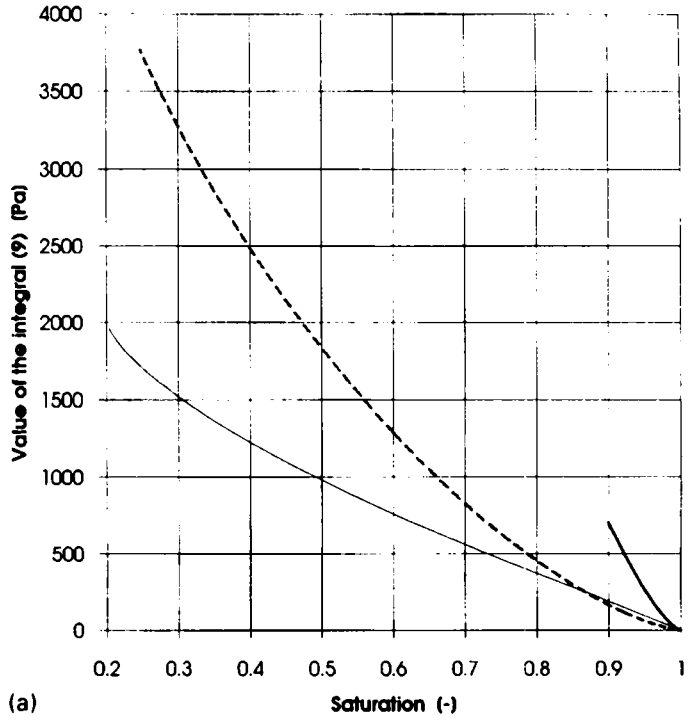

Figure 3. Comparison of properties of three different sands: (in (a) and (c) solid line indicates data according to Liakopoulos,[32] broken line — Safai and Pinder,[33] fine line – Brooks and Corey[34]. (a) Dependence of the integral term (9) upon the saturation; (b) pressure in the solid phase, according to Coussy (fine line) and Bishop (solid line), assuming $p_g = p_{atm}$ (1 indicates data according Safai and Pinder,[33] 2 — Liakopoulos,[32] 3 — Brooks and Corey[34]); (c) ratio of the above-mentioned pressure terms (the first one divided by the second one)

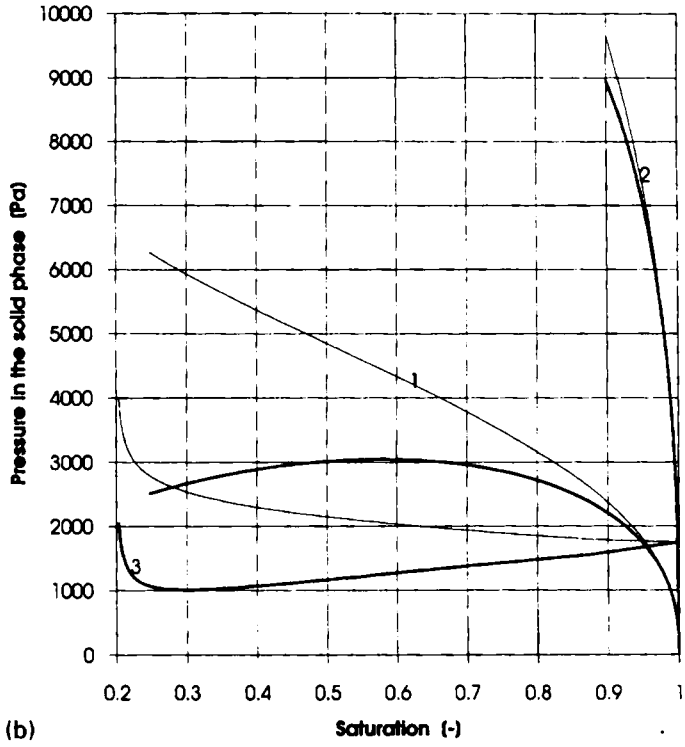

(b)

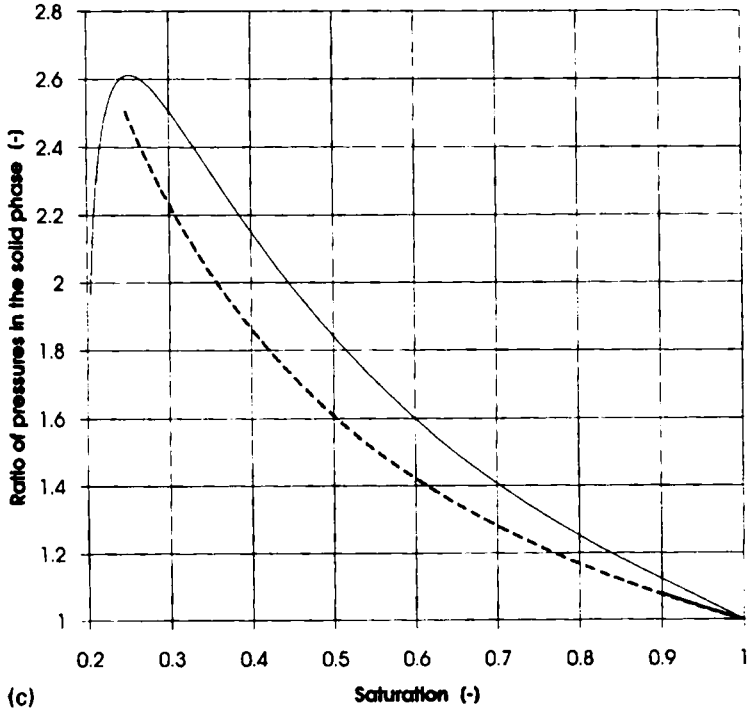

(c)

Figure 3. Continued

Energy conservation (enthalpy balance):

$$\rho C_p \frac{\partial T}{\partial t} + [C_{pw}\rho_w \mathbf{v}_\ell + C_{pg}\rho_{gw}\mathbf{v}_g]\cdot\nabla T - \nabla\cdot(\lambda_{eff}\nabla T) = \Delta h_{vap}\left[\phi\rho_\ell \frac{\partial S}{\partial t} + \alpha S\rho_\ell \frac{\partial}{\partial t}(\nabla\cdot\mathbf{u}) + \nabla\cdot(\rho_\ell \mathbf{v}_\ell)\right] \tag{12}$$

Linear momentum balance equation:

$$\nabla\cdot\sigma + \rho\mathbf{b} = 0 \tag{13}$$

or its time differentiated form

$$\nabla\cdot\dot{\sigma} + \dot{\rho}\mathbf{b} = 0 \tag{14}$$

where constant (time independent) specific body force $\mathbf{b}$ is assumed, ρ is the averaged density of the multiphase medium

$$\rho = (1-\phi)\rho_s + \phi S\rho_\ell + \phi(1-S)\rho_g \tag{15}$$

ϕ being the porosity, ρ_s the density of the solid, ρ_ℓ the density of the liquid water and ρ_g the density of the gas.

The constitutive relationship for the solid skeleton is here assumed in the form

$$\sigma' = \mathbf{D}_e(\varepsilon - \varepsilon^T) \tag{16}$$

where $\mathbf{D}_e$ is the elastic matrix, $\varepsilon^T = \frac{1}{3}\mathbf{I}\beta_s T$, is the strain caused by thermoelastic expansion and β_s means the cubic thermal expansion coefficient of the solid.

For fluid phases the multiphase *Darcy law* has been applied as constitutive equation, thus for liquid we have

$$\mathbf{v}_\ell = -\frac{\mathbf{K}K_{r\ell}}{\mu_\ell}(\nabla p_\ell - \rho_\ell \mathbf{b}), \quad p_c < p_b \tag{17a}$$

$$\mathbf{v}_\ell = -\frac{\mathbf{K}K_{r\ell}}{\mu_\ell}(\nabla p_g - \nabla p_c - \rho_\ell \mathbf{b}), \quad p_{cr} > p_c \geqslant p_b \tag{17b}$$

$$\mathbf{v}_\ell = \mathbf{0}, \quad p_c \geqslant p_{cr} \tag{17c}$$

while for the gas phase hold

$$\mathbf{v}_g = -\frac{\mathbf{K}K_{rg}}{\mu_g}\nabla p_g, \quad p_c \geqslant p_b \tag{18a}$$

$$\mathbf{v}_g = \mathbf{0}, \quad p_c < p_b \tag{18b}$$

where $\mathbf{K}$ is intrinsic permeability tensor, K_{rg} and $K_{r\ell}$ are relative permeabilities of the gaseous and liquid phase, $\mathbf{v}_\ell$ and $\mathbf{v}_g$ are the velocities of liquid and gaseous phase relative to the solid phase and the vector $\mathbf{b}$ indicates the specific body force term (normally corresponding to the acceleration of gravity).

Fick's law is applied for the description of the diffusion of the binary gas species mixture (dry air and water vapour):

$$\mathbf{v}_{ga}^d = -\frac{M_a M_w}{M^2} D_{eff}\nabla\left(\frac{p_{ga}}{p_g}\right) = \frac{M_a M_w}{M^2} D_{eff}\nabla\left(\frac{p_{gw}}{p_g}\right) = -\mathbf{v}_{gw}^d \tag{19}$$

Equation of state of perfect gases and *Dalton's law* are assumed for dry air (ga), vapour (gw) and moist air (g):

$$\begin{aligned} p_{ga} &= \rho_{ga} T\, R/M_a, \quad p_g = p_{ga} + p_{gw} \\ p_{gw} &= \rho_{gw} T\, R/M_w, \quad \rho_g = \rho_{ga} + \rho_{gw} \end{aligned} \tag{20}$$

For the solid skeleton the *effective stress principle* in its finite (4), incremental (6) or Coussy's formulation (7), accordingly to the analysed case, is here assumed.

Finally, for the closure of the model, some thermodynamic relations are used.

The *Kelvin equation* gives the relative humidity RH of the moist air inside the pores filled with water:

$$\mathrm{RH} = \frac{p_{gw}}{p_{gws}} = \exp\left(-\frac{p_c M_w}{\rho_\ell R T}\right), \tag{21}$$

where the water vapour saturation pressure p_{gws}, which depends only upon temperature T, can be obtained from the *Clausius–Clapeyron equation* or from empirical correlations, e.g. Reference 38.

It is further necessary to define the initial and boundary conditions.

The initial conditions specify the full fields of gas pressure, capillary pressure, temperature and displacement:

$$p_g = p_g^0, \quad p_c = p_c^0, \quad T = T^0, \quad \mathbf{u} = \mathbf{u}^0 \text{ at } t = 0 \tag{22}$$

The boundary conditions can be of the first kind or *Dirichlet BC* on Γ_i^1:

$$p_g = \hat{p}_g \text{ on } \Gamma_g^1, \quad p_c = \hat{p}_c \text{ on } \Gamma_c^1, \quad T = \hat{T} \text{ on } \Gamma_T^1, \quad \mathbf{u} = \hat{\mathbf{u}} \text{ on } \Gamma_u^1 \tag{23}$$

of the second kind or *Neumann BC* on Γ_i^2:

$$\begin{aligned} -(\rho_{ga}\mathbf{v}_g - \rho_g \mathbf{v}_{gw}^d)\cdot\mathbf{n} &= q_{ga} && \text{on } \Gamma_g^2 \\ -(\rho_{gw}\mathbf{v}_g + \rho_\ell \mathbf{v}_\ell + \rho_g \mathbf{v}_{gw}^d)\cdot\mathbf{n} &= q_{gw} + q_\ell && \text{on } \Gamma_c^2 \\ -(\rho_\ell \mathbf{v}_\ell \Delta h_{vap} - \lambda_{eff}\nabla T)\cdot\mathbf{n} &= q_T && \text{on } \Gamma_T^2 \\ \sigma\cdot\mathbf{n} &= \mathbf{t} && \text{on } \Gamma_u^2, \end{aligned} \tag{24}$$

and of the third kind or *Cauchy (mixed) BC* on Γ_i^3:

$$\begin{aligned} (\rho_{gw}\mathbf{v}_g + \rho_\ell \mathbf{v}_\ell + \rho_g \mathbf{v}_{gw}^d)\cdot\mathbf{n} &= \beta_c(\rho_{gw} - \rho_{gw\infty}) && \text{on } \Gamma_c^3 \\ (\rho_\ell \mathbf{v}_\ell \Delta h_{vap} - \lambda_{eff}\nabla T)\cdot\mathbf{n} &= \alpha_c(T - T_\infty) && \text{on } \Gamma_T^3 \end{aligned} \tag{25}$$

where the boundary $\Gamma = \Gamma_i^1 \cup \Gamma_i^2 \cup \Gamma_i^3$, $\mathbf{n}$ is the unit normal vector, pointing toward the surrounding gas, q_{ga}, q_{gw}, q_ℓ and q_T are, respectively, the imposed dry air flux, the imposed vapour flux, the imposed liquid flux and the imposed heat flux, and $\mathbf{t}$ is the imposed traction, $\rho_{gw\infty}$ and T_∞ are the mass concentration of water vapour and the temperature in the undisturbed gas phase distant from the interface, while α_c and β_c are convective heat and mass transfer coefficients.

3.1. *Numerical solution*

Discretization in space of the governing equations is carried out by means of the finite element method. The notations of Zienkiewicz and Taylor,[39,40] are used in the following, together with vector notation. The unknown variables are expressed in terms of their nodal values as

$$\begin{aligned} p_g &= p_g(t) = \mathbf{N}_p \bar{\mathbf{p}}_g(t), \quad p_c = p_c(t) = \mathbf{N}_p \bar{\mathbf{p}}_c(t) \\ T &= T(t) = \mathbf{N}_t \bar{\mathbf{T}}(t), \quad \mathbf{u} = \mathbf{u}(t) = \mathbf{N}_u \bar{\mathbf{u}}(t) \end{aligned} \tag{26}$$

The integral or weak form of the heat and mass transfer equations (and of the other ones required to complete the model), obtained by means of the Galerkin procedure[14,39,40] (weighted residuals) can be expressed in matrix form as[29,36]

$$\begin{aligned} &\mathbf{C}_{gg}\dot{\bar{\mathbf{p}}}_g + \mathbf{C}_{gc}\dot{\bar{\mathbf{p}}}_c + \mathbf{C}_{gt}\dot{\bar{\mathbf{T}}} + \mathbf{C}_{gu}\dot{\bar{\mathbf{u}}} + \mathbf{K}_{gg}\bar{\mathbf{p}}_g + \mathbf{K}_{gc}\bar{\mathbf{p}}_c + \mathbf{K}_{gt}\bar{\mathbf{T}} + \mathbf{f}_g = \mathbf{0}, \\ &\mathbf{C}_{cg}\dot{\bar{\mathbf{p}}}_g + \mathbf{C}_{cc}\dot{\bar{\mathbf{p}}}_c + \mathbf{C}_{ct}\dot{\bar{\mathbf{T}}} + \mathbf{C}_{cu}\dot{\bar{\mathbf{u}}} + \mathbf{K}_{cg}\bar{\mathbf{p}}_g + \mathbf{K}_{cc}\bar{\mathbf{p}}_c + \mathbf{K}_{ct}\bar{\mathbf{T}} + \mathbf{f}_c = \mathbf{0}, \\ &\mathbf{C}_{tg}\dot{\bar{\mathbf{p}}}_g + \mathbf{C}_{tc}\dot{\bar{\mathbf{p}}}_c + \mathbf{C}_{tt}\dot{\bar{\mathbf{T}}} + \mathbf{C}_{tu}\dot{\bar{\mathbf{u}}} + \mathbf{K}_{tg}\bar{\mathbf{p}}_g + \mathbf{K}_{tc}\bar{\mathbf{p}}_c + \mathbf{K}_{tt}\bar{\mathbf{T}} + \mathbf{f}_t = \mathbf{0}, \end{aligned} \tag{27}$$

Using the principle of virtual work and taking into account the boundary conditions (24)–(25), the linear momentum balance equation (13a) can be written in a weak form as[14,29,36]

$$-\int_\Omega \mathbf{B}^T \sigma' \, d\Omega + \mathbf{K}_{ug}\bar{\mathbf{p}}_g + \mathbf{K}_{uc}\bar{\mathbf{p}}_c + \mathbf{K}_{ut}\bar{\mathbf{T}} + \mathbf{f}_u = \mathbf{0} \tag{28a}$$

while its time differentiated form is

$$-\int_\Omega \mathbf{B}^T \dot{\sigma}' \, d\Omega + \mathbf{K}_{ug}\dot{\bar{\mathbf{p}}}_g + \mathbf{K}'_{uc}\dot{\bar{\mathbf{p}}}_c + \mathbf{K}'_{ut}\dot{\bar{\mathbf{T}}} + \dot{\mathbf{f}}_u = \mathbf{0} \tag{28b}$$

All the matrices occurring (27) and (28) are listed in References 29 and 36.

The above non-symmetric, non-linear and coupled system of ordinary differential equations can be rewritten in compact form as

$$\mathbf{C}(\mathbf{x})\dot{\mathbf{x}} + \mathbf{K}(\mathbf{x})\mathbf{x} + \mathbf{f}(\mathbf{x}) = \mathbf{0} \tag{29}$$

where

$$\mathbf{x}^T = \{\bar{\mathbf{p}}_g, \bar{\mathbf{p}}_c, \bar{\mathbf{T}}, \bar{\mathbf{u}}\}$$

and the non-linear (matrix) coefficients $\mathbf{C}(\mathbf{x})$, $\mathbf{K}(\mathbf{x})$ and $\mathbf{f}(\mathbf{x})$ are obtained by assembling the submatrices indicated in (27) and (28).

The time discretization is accomplished through a fully implicit finite difference scheme[39,40] (backward difference):

$$\mathbf{A}\mathbf{x}_{n+1} - \mathbf{B}\mathbf{x}_n - \mathbf{F} = \mathbf{0} \tag{30}$$

where

$$\begin{aligned} \mathbf{A} &= \mathbf{C}(\mathbf{x}_{n+1}) + \mathbf{K}(\mathbf{x}_{n+1})\Delta t \\ \mathbf{B} &= \mathbf{C}(\mathbf{x}_{n+1}) \\ \mathbf{F} &= -\mathbf{f}(\mathbf{x}_{n+1})\Delta t \end{aligned}$$

n being the time step number and Δt the time step length.

Considering the non-linearity of the system of equation (30) the solution is obtained with a Newton–Raphson type procedure:

$$\frac{1}{\Delta t}\left[\frac{\partial}{\partial \mathbf{x}}\mathbf{C}(\mathbf{x}_{n+1}^{l})(\mathbf{x}_{n+1}^{l}-\mathbf{x}_{n})+\mathbf{C}(\mathbf{x}_{n+1}^{l})\right]\Delta\mathbf{x}_{n+1}^{l}$$
$$+\left[\frac{\partial}{\partial \mathbf{x}}\mathbf{K}(\mathbf{x}_{n+1}^{l})\mathbf{x}_{n+1}^{l}+\mathbf{K}(\mathbf{x}_{n+1}^{l})+\frac{\partial}{\partial \mathbf{x}}\mathbf{f}(\mathbf{x}_{n+1}^{l})\right]\Delta\mathbf{x}_{n+1}^{l} \tag{31}$$
$$=-\left[\mathbf{C}(\mathbf{x}_{n+1}^{l})\frac{\mathbf{x}_{n+1}^{l}-\mathbf{x}_{n}}{\Delta t}+\mathbf{K}(\mathbf{x}_{n+1}^{l})\mathbf{x}_{n+1}^{l}+\mathbf{f}(\mathbf{x}_{n+1}^{l})\right]$$

where l is the iteration index, and at the end of each iteration the primary variables are updated as follows:

$$\mathbf{x}_{n+1}^{l+1}=\mathbf{x}_{n+1}^{l}+\Delta\mathbf{x}_{n+1}^{l} \tag{32}$$

A special 'switching' procedure,[36] allowing to deal with fully and partially saturated medium present at the same time in different parts of the domain, is applied.

Based on the presented discretization, the HMTRA-DEF research computer code has been developed[29,36] for the solution of the non-linear and non-symmetrical system of equations governing heat and mass transfer in a deformable porous medium. It has been partly modified as compared to its previous version[29,36] to be able deal with different time-differentiated formulations of the effective stress principle.

4. NUMERICAL EXAMPLES

To analyse practical effects of the different formulations of the effective stress principle on the results of computations, as well as on their numerical behaviour, two initial-boundary value problems are solved. The first deals with a fast desaturation process of a sand. For such a process the influence of these different formulations should be the biggest, thus also the easiest to analyse. The second, concerning a non-isothermal consolidation, was chosen to analyse a combined effect of distributed loads and temperature changes on the results obtained using different forms of the equilibrium equation. One cycle of saturation – desaturation is considered in this example. The histories of water and gas pressures and saturation are evidenced in each case. These histories influence the displacement field and are in turn influenced by it.

4.1. Desaturation example

This example is based on the experiment conducted by Liakopoulos on isothermal drainage of water from a vertical column of sand.[32] It was previously solved by Narasimhan and Witherspoon,[41] Schrefler and Simoni,[42] Zienkiewicz *et al.*,[27] Schrefler and Zhan,[31] Gawin *et al.*,[29] and Gawin and Schrefler.[36]

In this experiment a column of Perspex, 1 m high, was packed with Del Monte sand and instrumented to measure the moisture tension at several points along the column. Before the start of the experiment ($t < 0$), water was continuously added from the top and was allowed to drain freely at the bottom through a filter, until uniform flow conditions were established. At $t = 0$ the water supply was ceased and the tensiometer readings were recorded. The porosity, $\phi = 29.75$ per cent, and hydraulical properties of Del Monte sand were measured by Liakopoulos[32] by an independent set of experiments.

For numerical purposes the column was simulated by 20 eight-node isoparametric finite elements of equal size, the same for the pressures, temperature and displacement fields. A 3×3 Gauss' integration scheme was applied. During first 3600 s the time step $\Delta\tau = 1$ s was used, then $\Delta\tau = 10$ s till the end of the computations. The same convergence criterion was used for all the analysed cases; thus it was possible to compare the numerical behaviour of the different problem formulations on the basis of the iteration number and time step lengths necessary to obtain the converged solution (when convergence criterion was not fulfilled during 30 iterations, a two times smaller time step length was used).

At the beginning the hydrostatic water pressure distribution (i.e. unit vertical gradient of the potential and $p_c = 0$ on the top surface) and mechanical equilibrium state were assumed. The boundary conditions were the following: for the lateral surface, $q_T = 0$, $u_h = 0$, where u_h means horizontal displacement of soil; for the top surface, $p_g = p_{atm}$, $T = 293{\cdot}15$ K; for the bottom surface, $p_g = p_{atm}$, $p_c = 0$, $T = 293{\cdot}15$ K, $u_h = u_v = 0$, where u_v means vertical displacement of soil.

Liakopoulos did not measure the mechanical parameters of the soil, so its linear elastic behaviour was assumed with the Young modulus $E = 1{\cdot}3$ MPa, Poisson's ratio $v = 0{\cdot}4$ and Biot's constant as $\alpha = 1$, similarly as in References 29, 31 and 42.

During computations the approximated equations of the Liakopoulos' saturation–capillary pressure and relative permeability of water–capillary pressure relationships of the following form:

$$\begin{aligned} S &= 1 - 1{\cdot}9722 \cdot 10^{-11}\, p_c^{2{\cdot}4279} \\ K_{rl} &= 1 - 2{\cdot}207(1 - S)^{1{\cdot}0121} \end{aligned} \tag{33}$$

were applied.

The relative permeability of the gas phase was assumed according to the relationship of Brooks and Corey,[34]

$$\begin{aligned} K_{rg} &= (1 - S_e)^2(1 - S_e^{5/3}) \\ S_e &= (S - 0{\cdot}2)/(1 - 0{\cdot}2) \end{aligned} \tag{34}$$

with the additional lower limit $K_{rg} \geqslant 0{\cdot}0001$, which was necessary to avoid numerical problems arising during transition from fully to partially saturated state.[36] The 'switching' from fully to partially saturated solution was performed at $p_c = 0$ Pa, thus in the whole partially saturated zone of the medium two-phase flow was considered.

The initial-boundary problem was solved for the three cases corresponding to the different formulations of the effective stress relationship:

(i) Bishop's finite formulation (4),
(ii) Bishop's time-differentiated (incremental) formulation (6),
(iii) Coussy's time-differentiated (incremental) formulation (7b).

The resulting time histories of water pressure, saturation, capillary pressure, gas pressure and vertical displacements at four different heights $h = 0{\cdot}25$, $0{\cdot}5$, $0{\cdot}75$ and $1{\cdot}0$ m for the three considered cases are compared in Figures 4(a)–4(e)

The differences between the solutions for all the analysed cases are very small. Only during first 10 min, when transition from fully to partially saturated state takes place at successive heights (starting from the top), more distinct differences can be observed, especially in gas pressure profiles (the state variable most sensitive for oscillations). They are caused by small and quickly disappearing instabilities arising during 'switching' procedure for the time-differentiated formulation

of the equilibrium equation (14). In fact, the lower limit of gas relative permeability (which was assumed in order to avoid these osciliations[36]) was fitted for case (i) and was obviously not sufficient for the other cases. Figures 4(c) and 4(d) evidence a better numerical behaviour of the finite form of equation (13), which also needed less iterations to converge. Only vertical displacement profiles demonstrate some differences, which do not diminish with time. To evidence them better, in Figure 5(a) the vertical displacement histories for different heights during first 100 s and in Figure 5(b) at high $h = 1$ m for time values $t > 1000$ s have been presented. The mentioned differences between the solutions for the finite and the time-differentiated equilibrium equations (13) and (14) appear already after the first time step ($t = 1$ s) and then their magnitude is practically constant for all levels as long as that level remains fully saturated ($S = 1$, thus zero integral term (9) — Figure 3(a)). That difference is caused by the fact that in the time-differentiated formulation we have additional initial condition for the time derivative of state variables, which are assumed equal to zero. This produces smaller displacements during first time step.

Then, after a transient period, in which 'switching' from fully to partially saturated state occurs, and starting from about $\tau = 1000$ s, the difference between cases (i) and (ii) is still practically constant, while the difference between solutions for the two time-differentiated formulations increases, being still relatively small. The latter is caused by lack of the term with the saturation change rate in equation (7b) (Coussy's formulation) as compared with equation (6). It becomes

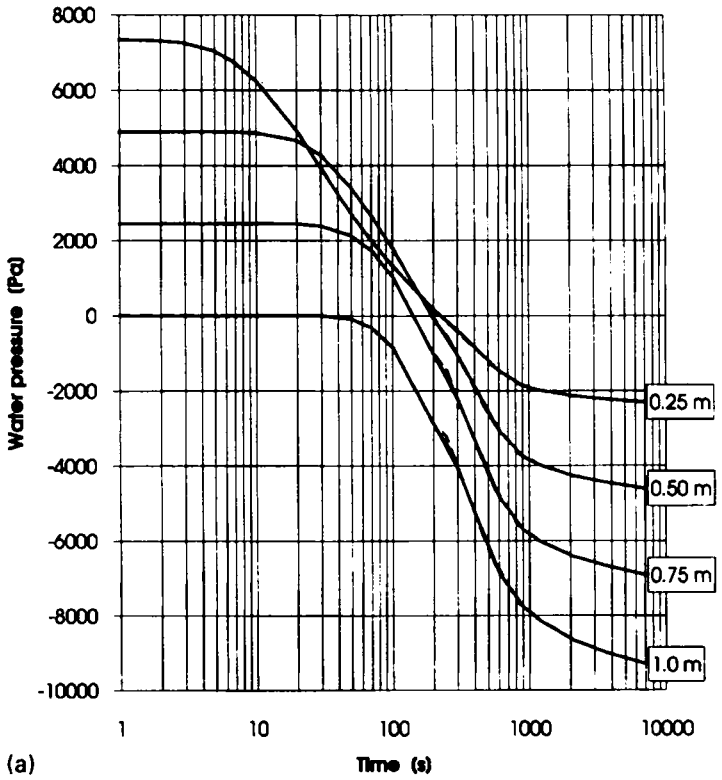

Figure 4. Comparison of the resulting time histories at four different heights (case (i) indicated by solid lines, case (ii) — fine lines, case (iii) — dotted line) during desaturation of the sand with data according to Liakopoulos.[32] (a) Water pressure (with respect to atmospheric pressure); (b) saturation; (c) capillary pressure (in fully saturated zone it means water pressure, negative capillary pressure has no meaning); (d) gas pressure; (e) vertical displacement

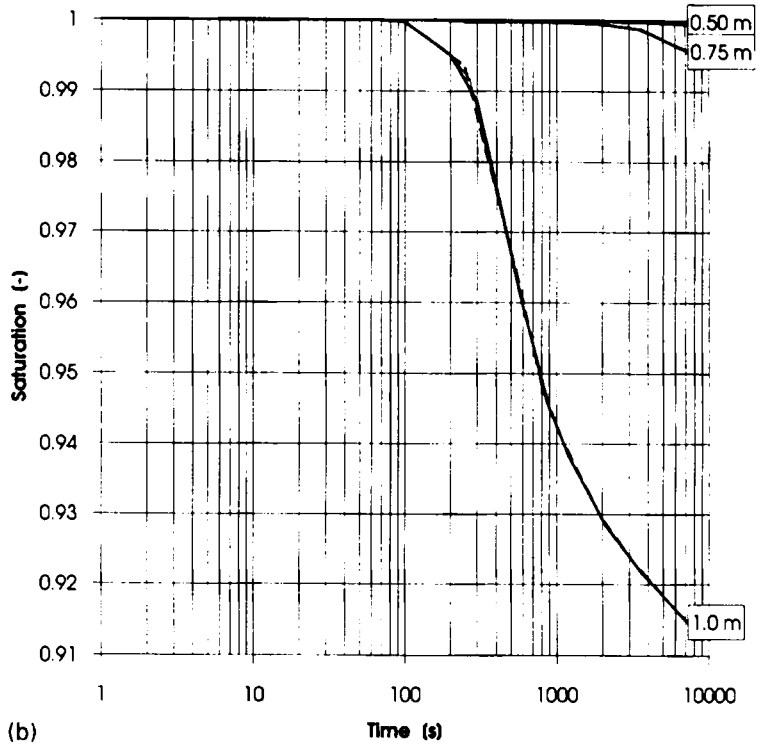

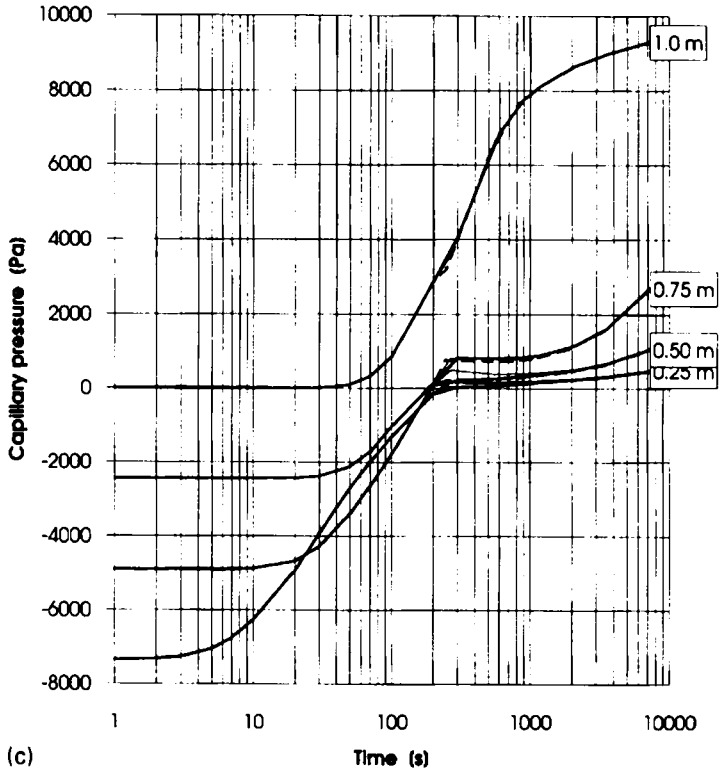

Figure 4. Continued

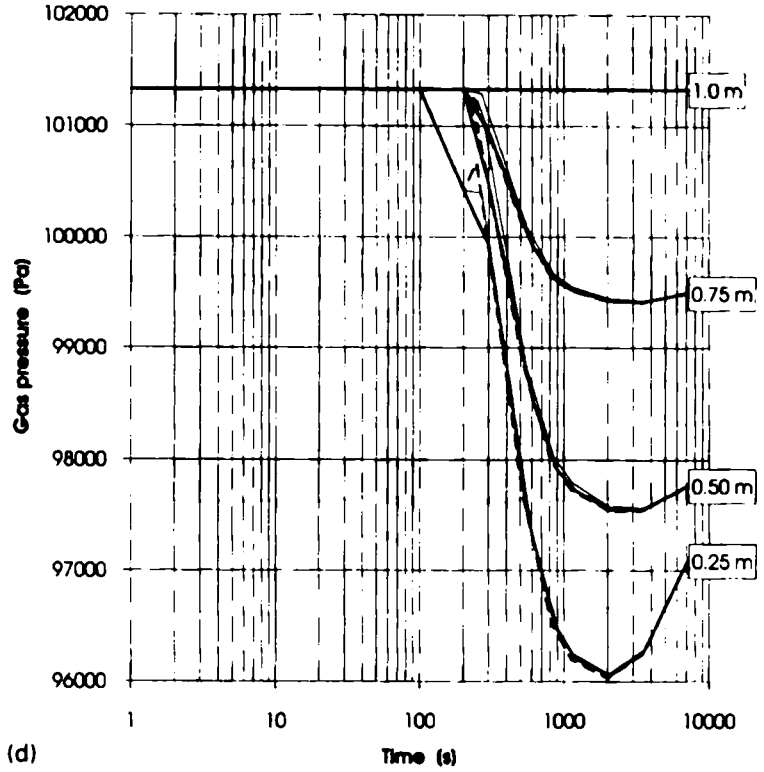

(d)

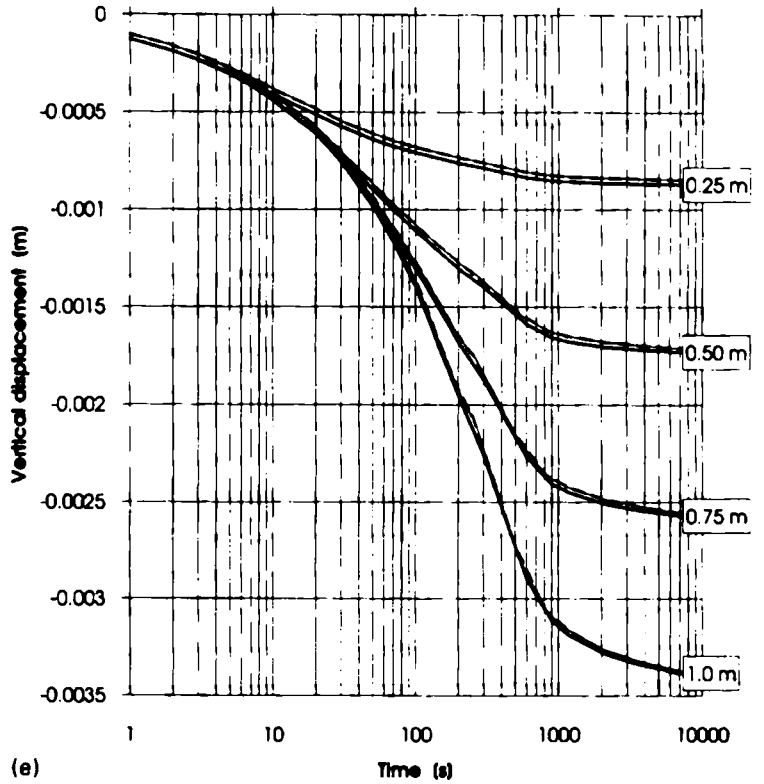

(e)

Figure 4. Continued

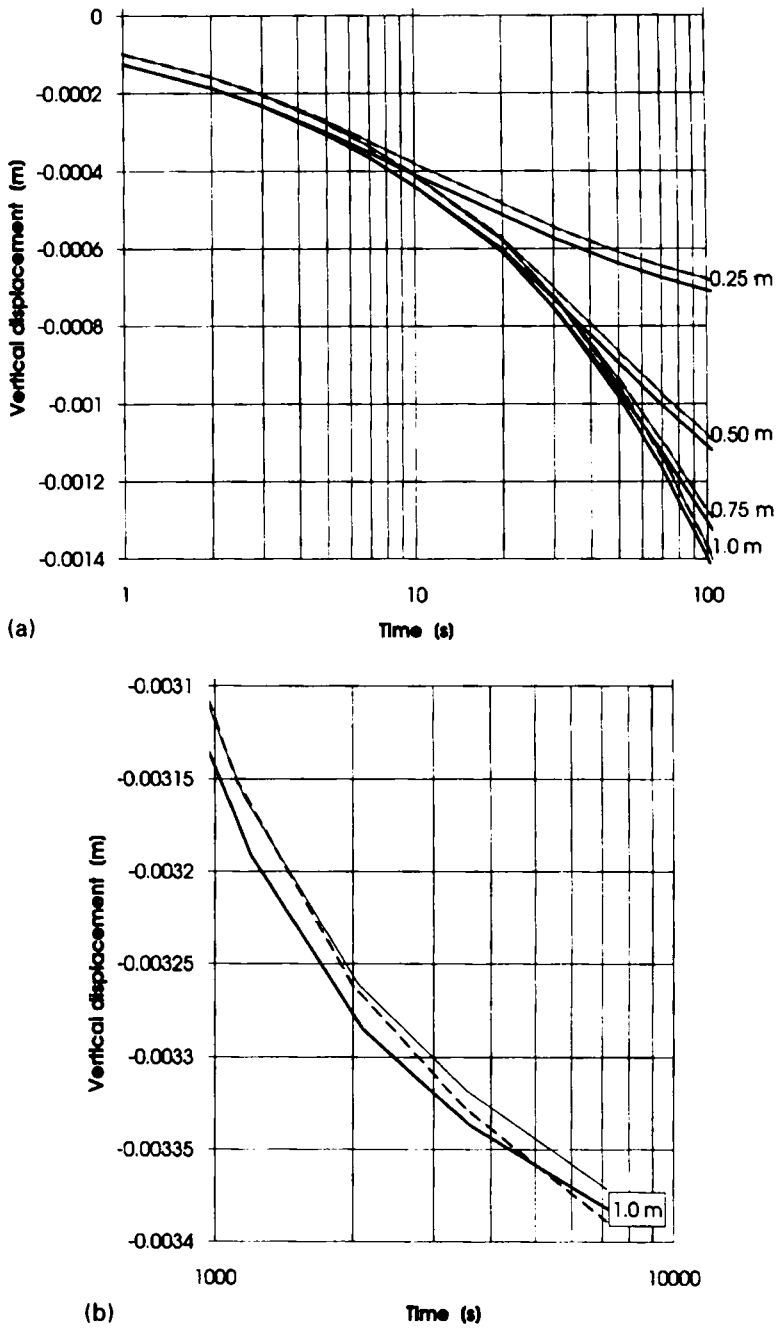

Figure 5. Detailed comparison of the resulting time histories of the vertical displacement: (case (i) indicated by solid lines, case (ii) — fine line, case (iii) — dotted line) during desaturation of the sand with data according to Liakopoulos.[32] (a) At four different heights during first 100 s; (b) at height $h = 1{\cdot}0$ m for $t > 1000$ s

more substantial when relatively fast desaturation of the upper part of the sand column occurs (Figure 4(b)).

To analyse the differences between the three formulations of the effective stress principle in the range of lower saturations, where these differences should be more evident, the same example, but using data of another sand[33] (dotted line in Figure 2), was solved. This is a sand which desaturates much more rapidly, see Figure 2 and compare Figures 4(b) and 7(b). In this case the higher value of the lower limit of the gas relative permeability $K_{rg} \geqslant 0{\cdot}0005$ was necessary to assure the converged solution. The initial and boundary conditions, as well as the finite element mesh were identical as before. A larger time step than in the previous case was necessary at early stages of the desaturation process to avoid oscillations during the transient from fully to partially saturated state. Thus, during first 5 h the time step $\Delta\tau = 10$ s was used, then $\Delta\tau = 20$ s during next 2 h, and finally $\Delta\tau = 60$ s till the end of the computations.

The resulting profiles of water pressure, saturation, capillary pressure and vertical displacement at different time stations for the three considered cases are compared in Figures 6(a)–6(e) while the corresponding time histories at four different heights are presented in Figures 7(a)–7(e). They show very small differences except for the vertical displacement profiles, especially at higher time values. Like in the previous example, some small, not diminishing differences between the solutions for finite, case (i), and incremental formulations, cases (ii) and (iii), can be observed

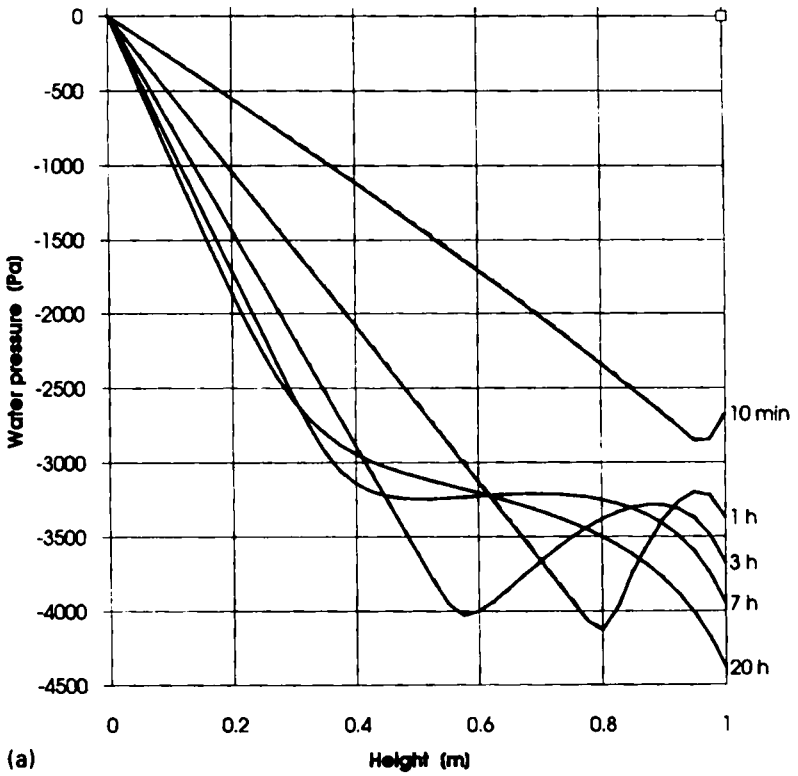

Figure 6. Comparison of the resulting profiles at five different time stations (case (i) indicated by solid lines, case (ii) — fine lines, case (iii) — dotted line) during desaturation of the sand with data according to Safai and Pinder.[33] (a) Water pressure (with respect to atmospheric pressure); (b) saturation; (c) capillary pressure; (d) gas pressure; (e) vertical displacement

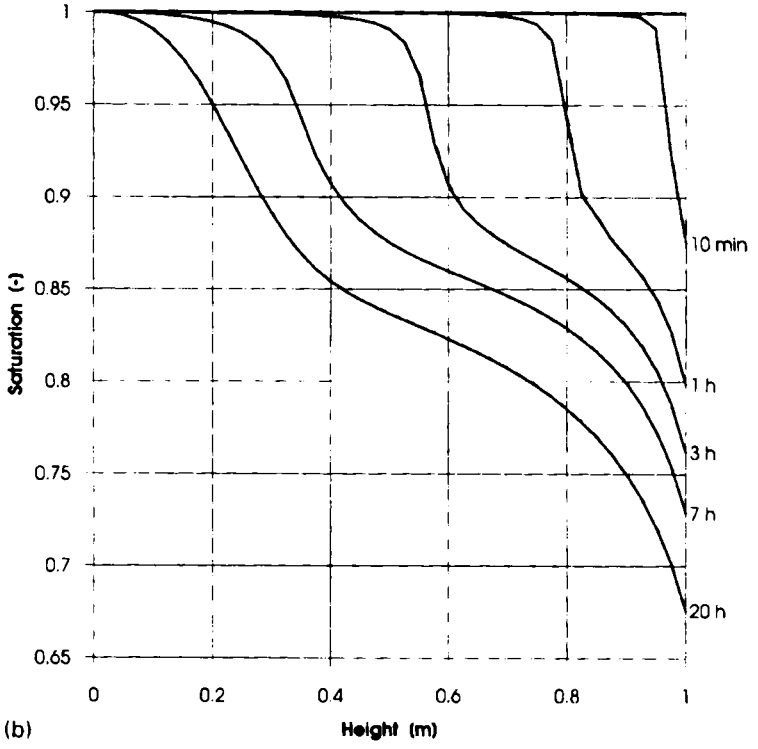

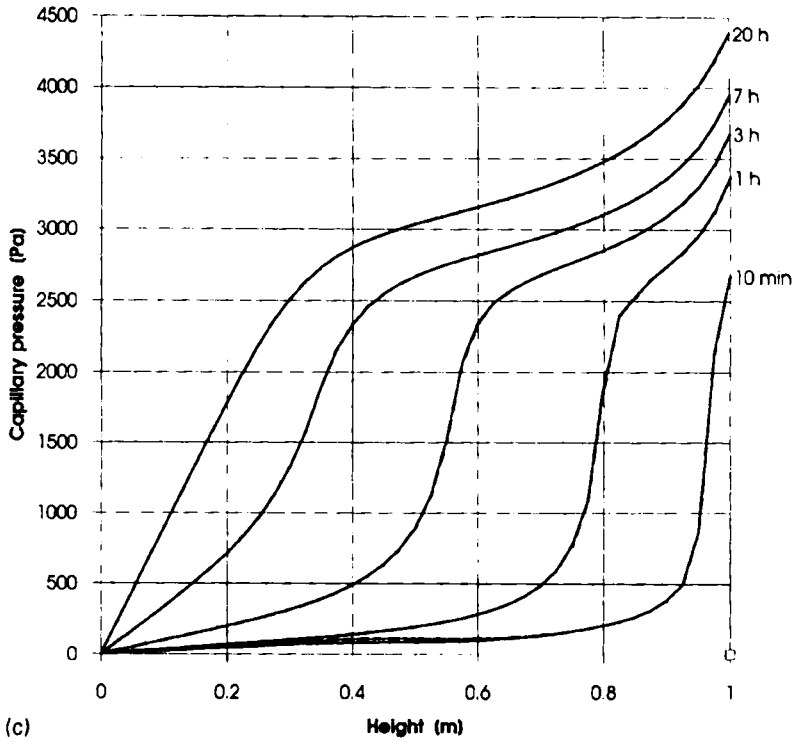

Figure 6. Continued

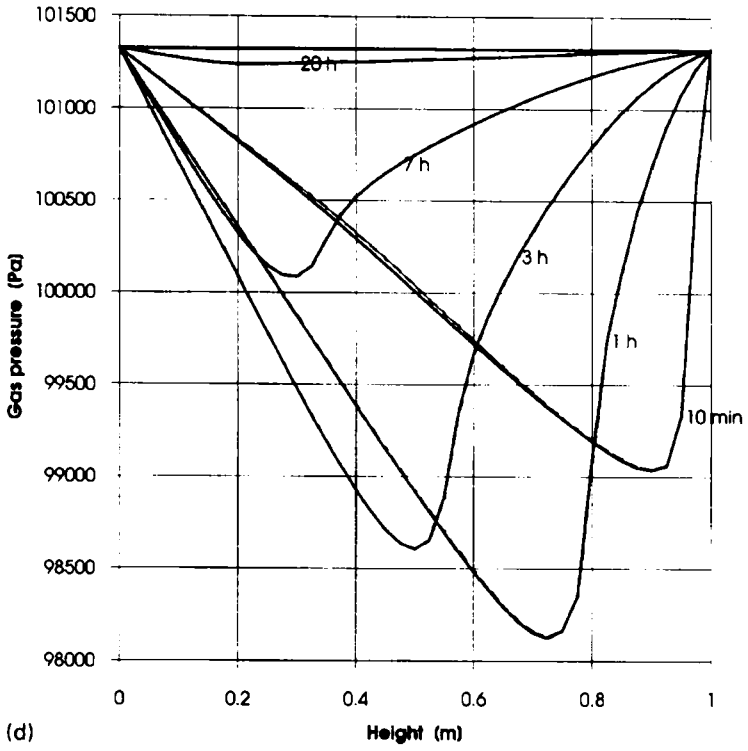

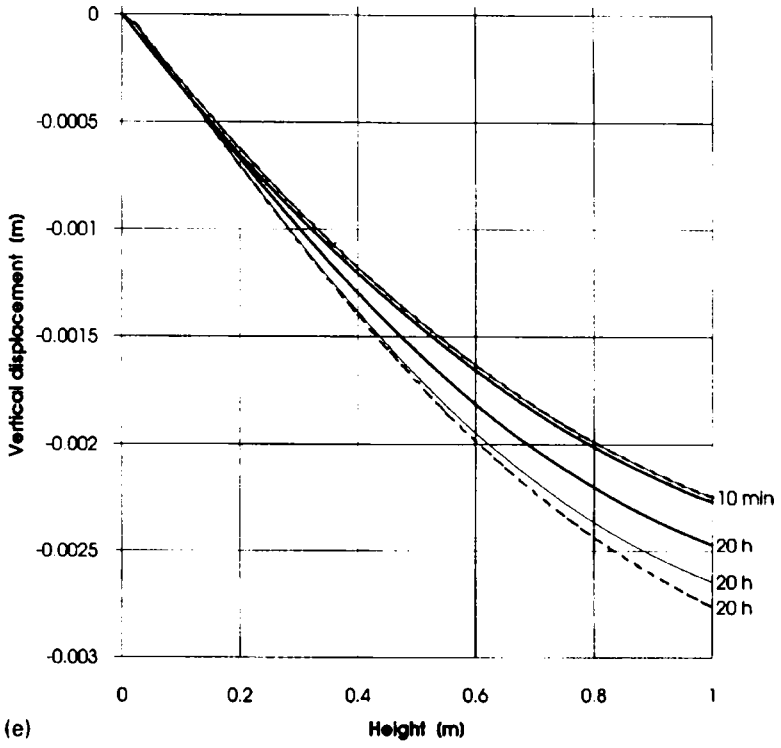

Figure 6. Continued

already after the first time step. Then they remain almost constant until the moment, when a fast desaturation process begins in a considerable part of the medium and they start to increase. In general, larger differences have been observed between cases (i) and (ii) (less than 8 per cent of the total displacement), then between the two incremental formulations (ii) and (iii) (less than 6 per cent). The difference between (i) and (ii) is due to the fact that the set of possible solution trajectories is modified through time differentiation.

In the medium a characteristic wave of higher pressure, moving from the top to the bottom of the column can be observed during the first hours (Figures 6(a) and 7(a)).

During computations in the model with the time-differentiated equilibrium equation some problems arise when a rapid change (of the type of Heaviside function) of boundary conditions occurs. In fact, the corresponding differentials have a shape like Dirac's delta function, what causes some numerical problems and can be a source of additional inaccuracies.

4.2. Non-isothermal consolidation

This example deals with thermoelastic consolidation of a partially saturated geomaterial. It was previously solved by Schrefler and Zhan[31] neglecting latent heat and phase change and then

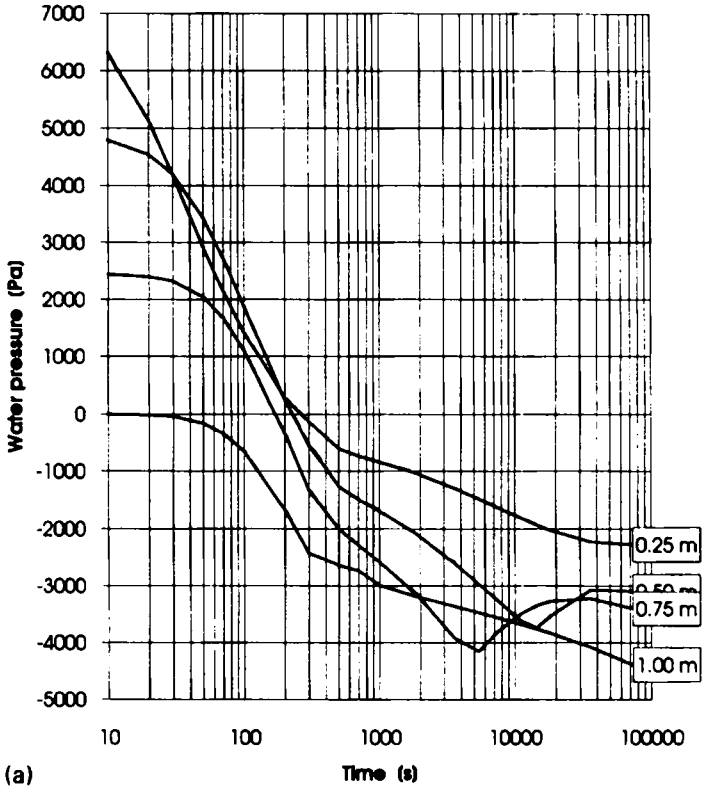

Figure 7. Comparison of the resulting time histories at four different heights (case (i) indicated by solid lines, case (ii) — fine lines, case (iii) — dotted line) during desaturation of the sand with data according to Safai and Pinder.[33] (a) Water pressure (with respect to atmospheric pressure); (b) saturation; (c) capillary pressure in fully saturated zone it means water pressure, negative capillary pressure has no meaning; (d) gas pressure; (e) vertical displacement

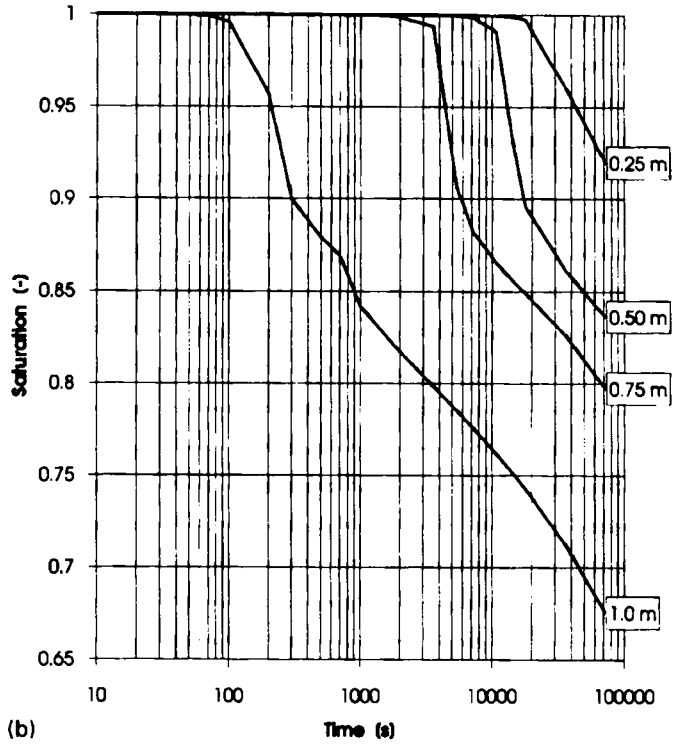

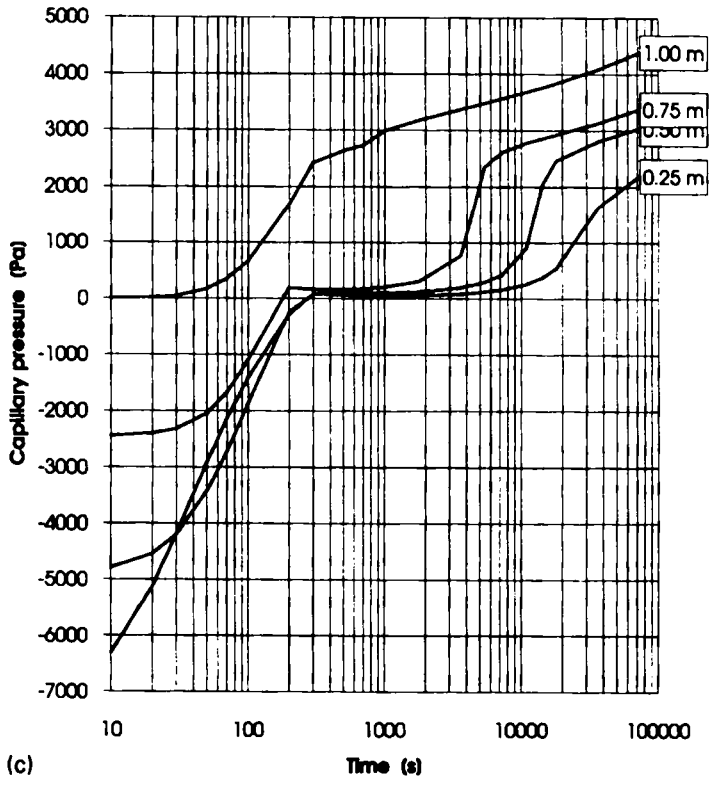

Figure 7. Continued

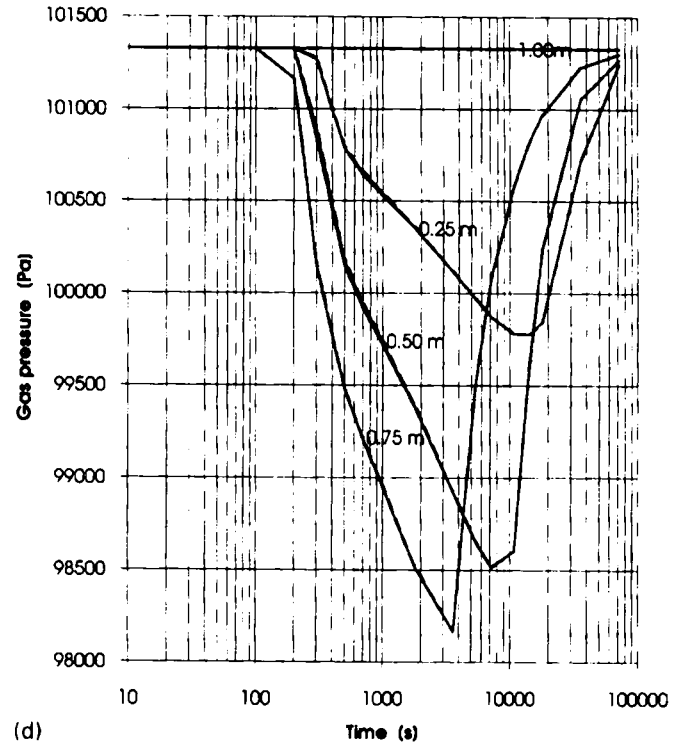

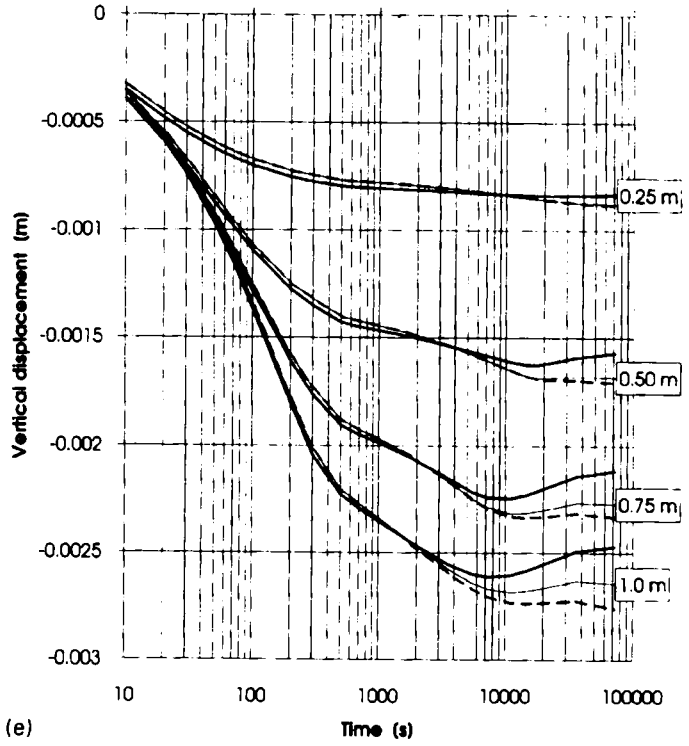

Figure 7. Continued

by Gawn *et al.*,[29] taking into account these two factors, which in advanced stages of the process have been shown to be of importance. Here this example is solved for the three different formulations of the momentum balance equation, like in the previous section and additionally, with respect to Reference 29, taking into account variation of the thermal capacity with water saturation of the medium to analyse all possible effects of these formulations.

In this example a column, of 7 m height, of linear elastic material which Young modulus $E = 6$ MPa and Poisson ratio $v = 0{\cdot}4$, was subjected to an external surface load of 1000 Pa and to a surface temperature jump of 50 K above the initial temperature of 293·15 K. The other data of the porous medium were assumed the same in References 14, 29 and 31. The relationships between capillary pressure, saturation of water and relative permeabilities of water and gas proposed by Brooks and Corey[34] were used. Water and solid phase were assumed incompressible.

The boundary conditions were the following: for the lateral surface, $q_T = 0$; $u_h = 0$; for the top surface, $T = 343{\cdot}15$ K, $p_g = p_{atm}$, $p_C = 0$ for fully saturated case or $p_C = p_C^*$ for partially saturated case, where p_C^* means capillary pressure corresponding to saturation $S = 0{\cdot}92$; for bottom surface, $q_T = 0$, $u_v = 0$. For numerical purposes the column was simulated by 18 (a two times finer mesh than in Reference 14, 29 and 31) eight-node isoparametric elements, the same for all state

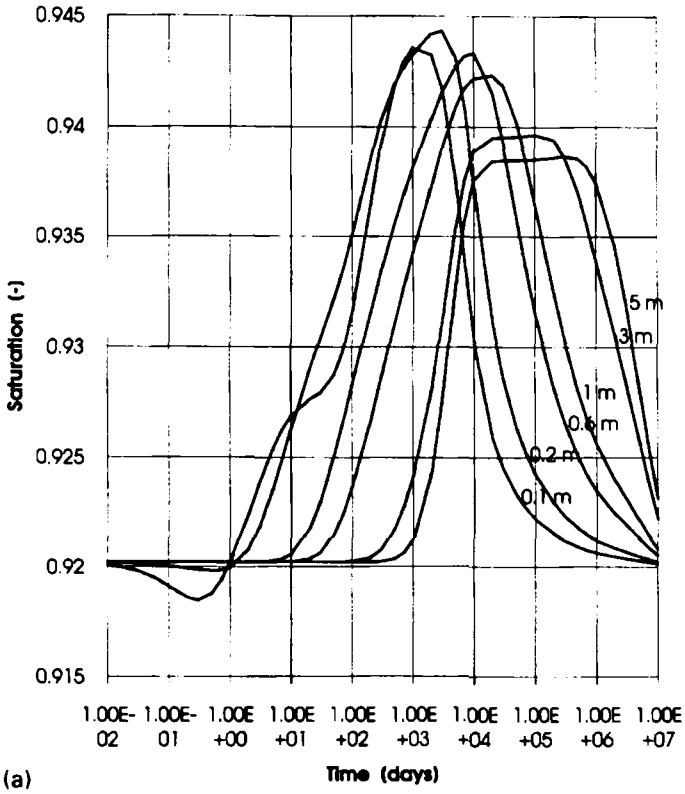

Figure 8. Comparison of the resulting histories at six different heights (case (i) indicated by solid lines, case (ii) — fine lines, case (iii) — dotted line) during non-isothermal consolidation of the sand with data according to Brooks and Corey.[34] (a) saturation; (b) temperature; (c) capillary pressure; (d) vertical displacement

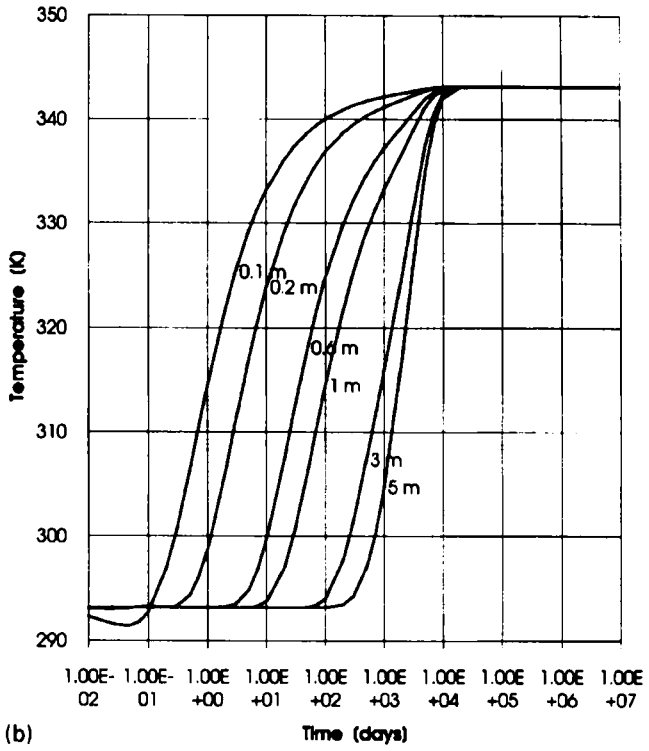

(b)

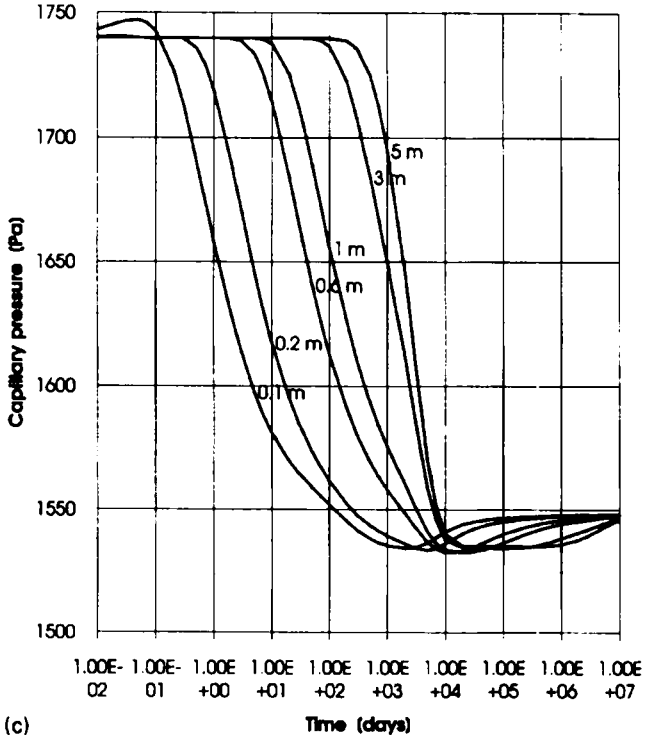

(c)

Figure 8. Continued

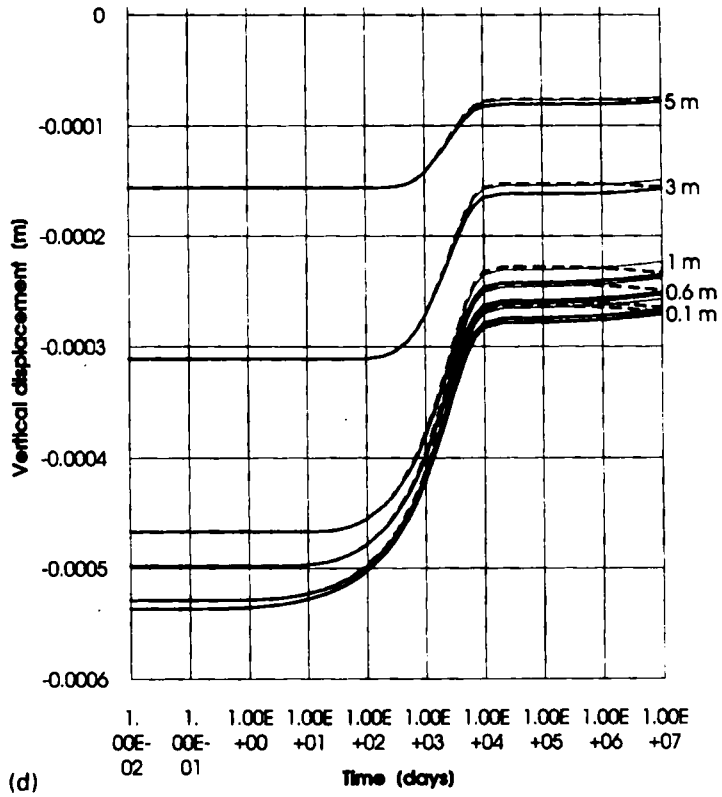

Figure 8. Continued

variables. A 3 × 3 Gaussian integration scheme was used. Temporal discretization was performed with an initial step of 0·01 days during the first 100 steps and multiplied by 10 after repeating 90 steps until 10^7 days, the final time of the simulations. Similarly as in the previous example, the same convergence criterion was used for all the analysed cases.

The problem was solved for initially homogenous saturation of water $S = 0{\cdot}92$ and modified, temperature-dependent, capillary pressure–saturation relationship of Brooks and Corey.[34] It was assumed that this relationship was measured at a temperature $T = 293{\cdot}15$ K and a change of capillary pressure due to dependence of surface tension on temperature[43] was introduced.

The example is difficult from numerical point of view, particularly for the shape of the capillary pressure–saturation relationship of Brooks and Corey.[34] At the beginning of the simulation some unstable behaviour of temperature and pressure solutions (especially for time-differentiated formulations (ii) and (iii) in a region close to the surface was observed, where a rapid change of the temperature was imposed as boundary condition. To avoid these oscillations which could influence the obtained results and give false conclusions about real effect of the effective stress formulation, the gas pressure in the whole column was assumed equal to atmospheric pressure value. This is a common assumption in soil mechanics.[27]

The comparison of the resulting time histories of saturation, temperature, capillary pressure and vertical displacements, at different distances $x = 0{\cdot}1, 0{\cdot}2, 0{\cdot}6, 1, 3$ and 5 m from the top surface of the column, for the case (i)–(iii), is shown in Figures 8(a)–8(d). Similarly as in the previous example almost no differences for saturation, temperature and capillary pressure fields have been

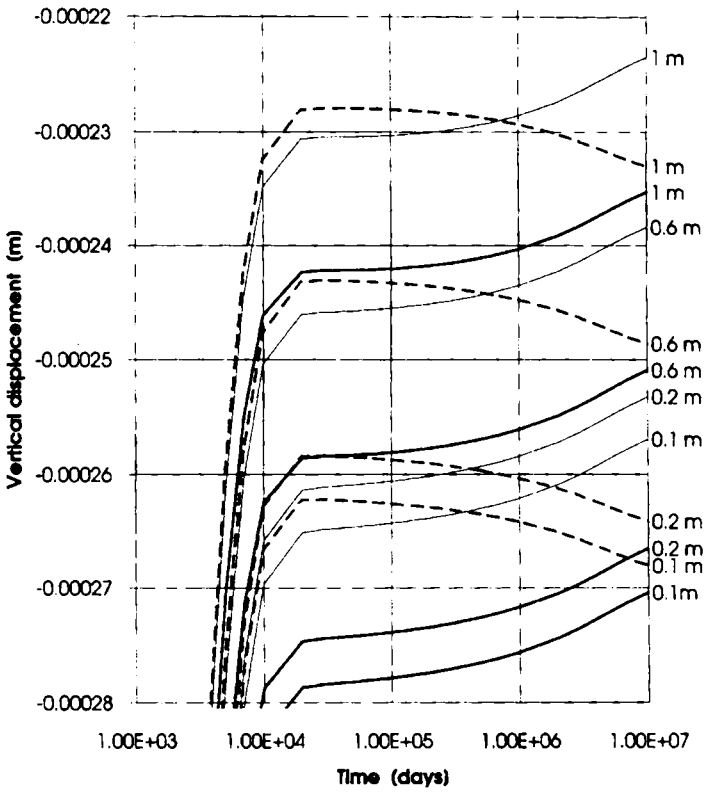

Figure 9. Detailed comparison of the resulting time histories of the vertical displacement: (case (i) indicated by solid line, case (ii) — fine lines, case (iii) — dotted line) during non-isothermal consolidation of the sand with data according to Brooks and Corey[34]

observed. Only results for the vertical displacement have shown some differences increasing in time, between the three individual analysed cases. They appear when a higher temperature front reaches deeper parts of the medium, causing its swelling, and become more evident when saturation changes due to condensation and following evaporation. To evidence these differences, in Figure 9 the displacement histories in four points close to the surface are presented in detail. A quantitatively different behaviour of the solution for the case (iii), as compared to the cases (i) and (ii), could be observed. It is caused by the lack in Coussy's formulation of the effective stress principle (7b) of the term containing the saturation change rate, which is of importance at advanced stages of the simulation (Figure 8(a)). Nevertheless, the biggest observed differences, occurring between the solutions for the cases (i) and (iii), do not exceed 5 per cent, even for very high time values (10^7 days).

5. CONCLUSIONS

The different formulations for the effective stress principle stem from different models and assumptions. Therefore, it is not easy to reach an agreement. Stress–strain relationships can be obtained for the effective stress coming from both investigated forms. Hence, also from there no clear answer can be expected. It has been shown that in unsaturated case formal differences arise

which yield different linear momentum balance equations of the multiphase medium, because the incremental form of the effective stress principle is not an exact differential. The assumed capillary pressure–saturation relationship has been shown to play an important role in these differences. Numerical experiments on initial-boundary value problems however show that in practical soil mechanics situations the resulting differences are small and appear usually after long lasting variation of the moisture content. Only several cycles of wetting and drying would produce significant differences.

From the computational point of view it is more convenient to adopt the finite form of the effective stress principle. This advantage should be more important when also dynamic situations have to be taken into account.

ACKNOWLEDGEMENTS

This work has been carried out within the framework of HCM Project ALERT Geomaterials and was partly financed by the Italian Ministry of Scientific and Technological Research (MURST 40 per cent).

The second author's research has been supported by TEMPUS PHARE Project.

APPENDIX I

Nomenclature

$\mathbf{B}$	strain matrix relating strain and displacement
$\mathbf{b}$	specific body force, $m\,s^{-2}$
C_p	effective specific heat of the porous medium, $J\,kg^{-1}\,K^{-1}$
C_{pg}	specific heat of the gas mixture, $J\,kg^{-1}\,K^{-1}$
C_{ps}	specific heat of the solid matrix, $J\,kg^{-1}\,K^{-1}$
C_{pl}	specific heat of the liquid phase (water), $J\,kg^{-1}\,K^{-1}$
$\mathbf{D}_e$	elastic matrix, Pa
D_{eff}	effective diffusivity of the gas mixture, $m^2\,s^{-1}$
E	Young modulus, Pa
$\mathbf{I}$	unit tensor
$\mathbf{K}$	intrinsic permeability tensor, m^2
K_S	bulk modulus of the solid phase, Pa
K_T	bulk modulus of the porous medium Pa
K_{rg}	relative permeability of the gas phase, dimensionless
K_{rl}	relative permeability of the liquid phase, dimensionless
k	hydraulic conductivity, $m\,s^{-1}$
M	molar mass of the gas moisture (moist air), $kg\,kmol^{-1}$
M_a	molar mass of the dry air, $kg\,kmol^{-1}$
M_w	molar mass of the water vapour, $kg\,kmol^{-1}$
$\mathbf{n}$	unit normal vector
p	average pressure of the mixture, Pa
p_{atm}	atmospheric pressure, Pa
p_b	bubbling pressure, Pa
p_c	capillary pressure, Pa
p_{cr}	critical value of capillary pressure, Pa
p_g	pressure of the gas phase, Pa

p_{gw} water vapour partial pressure, Pa
p_{gws} water vapour saturation pressure, Pa
p_l liquid water pressure, Pa
q_{ga} dry air flux imposed on the boundary
q_{gw} vapour flux imposed on the boundary
q_l liquid flux imposed on the boundary
q_T heat flux imposed on the boundary
R gas constant (8314.41 J kmol^{-1} K^{-1})
S liquid-phase volumic saturation (liquid Vol./pore Vol.)
T temperature, K
T_∞ temperature in the undisturbed gas phase distance from the interface, K
t time, s
$\mathbf{t}$ traction imposed on the boundary, Pa
$\mathbf{u}$ displacement vector of the solid matrix, m
u_h horizontal displacement, m
u_v vertical displacement, m
$\mathbf{v}_g$ velocity of the gaseous phase, m s^{-1}
$\mathbf{v}_l$ velocity of the liquid phase, m s^{-1}
$\mathbf{v}_{ga}^d$ relative average diffusion velocity of dry air species, m s^{-1}
$\mathbf{v}_{gw}^d$ relative average diffusion velocity of water vapour species, m s^{-1}

Greek symbols

α Biot's constant
α_c convective heat transfer coefficient, W m^{-2} K^{-1}
β_c convective mass transfer coefficient, m s^{-1}
β_s cubic thermal expansion coefficient of the solid K^{-1}
Δh_{vap} specific enthalpy of evaporation, J kg^{-1}
$\Delta t, \Delta\tau$ time step, s
ε elastic strain
ε^T thermoelastic strain
ε_v volumetric strain
Γ_i^1 part of the boundary Γ, where BC of the first kind are applied for the i-variable (the imposed value of i-variable)
Γ_i^2 part of the boundary Γ, where BC of the second kind are applied for i-variable (the imposed value of flux corresponding to the i-variable)
Γ_i^3 part of the boundary Γ, where BC of the third kind are applied for the i-variable (the imposed value of the i-variable and of flux corresponding to it)
λ_{eff} effective thermal conductivity, W m^{-1} K^{-1}
μ_g gas-phase dynamic viscosity, Pa s
μ_l liquid-phase dynamic viscosity, Pa s
ν Poisson's ratio, dimensionless
ρ effective density of the porous medium, kg m^{-3}
ρ_g gas-phase density, kg m^{-3}
ρ_{ga} mass concentration of dry air in the gas phase, kg m^{-3}
ρ_{gw} mass concentration of water vapour in the gas phase, kg m^{-3}
$\rho_{gw\infty}$ mass concentration of water vapour in the undisturbed gas phase distant from the interface, kg m^{-3}

ρ_f liquid-phase density, kg m^{-3}
σ total stress tensor, Pa
σ' effective stress tensor, Pa
ϕ porosity [pore Vol./total Vol.]

REFERENCES

1. A. W. Skempton, 'Effective stress in soils, concrete and rock', *Proc. Conf. on Pore Pressure and Suction in Soils*, Butterworth, 1960, pp. 4–16.
2. P. V. Lade, and R. de Boer, 'The concept of effective stress for soil, concrete and rock', *Geotechnique*, to appear.
3. K. Terzaghi, 'The shearing resistance of saturated soils and the angle between the planes of shear', *First Int. Conf. on Soil Mech. and Found. Engr.*, Harvard University, Vol. I, 1936, pp. 54–56.
4. P. Fillunger, 'Versuche ueber die Zugfestigkeit bei allseitigem Wasserdruck', *Oesterr. Wochenschrift oeffent. Baudienst*, **29**, 443–448 (1915).
5. M. A. Biot, 'General theory of three-dimensional consolidation', *J. Applied Phys.*, **12**, 155–164 (1941).
6. F. Gassman, 'Ueber die Elastizitaet poroeser Medien', *Vierteljahrschrft Naturforschenden der Gesellschaft Zuerich*, **96**, 1–23 (1951).
7. M. A. Biot and D. G. Willis, 'The elastic coefficients of the theory of consolidation', *J. Appl. Mech.* **24**, 594–601 (1957).
8. J. Geertsma, 'The effect of fluid pressure decline on volumetric changes of porous rocks', *Trans. AIME*, **210**, 331–340 (1957).
9. J. Geertsma, 'Problems of rock mechanics in petroleum production engineering', *Proc. 1st Int. Congr. Rock Mechanics*, Lisbon, Vol. I, R. 359, 1966, p. 585.
10. J. L. Serafim, 'The 'uplift area' in plain concrete in the elastic range', *Proc. 8th Congr. on Large Dams*, Edinbourgh, Vol. V, C. 17, 1964.
11. A. Nur and J. D. Byerlee, 'An exact effective stress law for elastic deformation of rock with fluids', *J. Geophys. Res.* **76**, 6414–6419 (1971).
12. A. W. Bishop, 'The influence of an undrained change in stress on the pore pressure in porous media of low compressibility', *Geotechnique*, **23**, 435–442 (1973).
13. A. W. Bishop, 'The principle of effective stress', *Teknisk Ukeblad*, **39**, 859–863 (1959).
14. R. W. Liews and B. A. Schrefler, *The Finite Element Method in the Deformation and Consolidation of Porous Media*, Wiley and Sons, Chichester, 1987.
15. M. Hassanizadeh and W. G. Gray, 'General conservation equations for multiphase systems: 1. Averaging technique, *Adv. Water Res.*, **2**, 131–144 (1979). 2. Mass, momenta, energy and entropy equations, *Adv. Water Res.*, **2**, 191–203 (1979). 3. constitutive theory for porous media flow', *Adv. Water Res.*, **3**, 25–40 (1980).
16. B. D. Coleman and W. Noll, 'The thermodynamics of elastic materials with heat conduction and viscosity', *Arch. Ration. Mech. Anal.*, **13**, 168–178 (1963).
17. G. Gudehus, 'A comprehensive concept for non-saturated granular bodies', in *Unsaturated Soils/Sols Non Saturés*, E. E. Alonso and P. Delage (eds), Balkeman, Rotterdam, 1995, pp. 725–737.
18. G. Bolzon and B. A. Schrefler, 'State surfaces of partially saturated soils: an effective pressure approach', *Appl. Mech. Rev.*, **48**, 643–649 (1995).
19. G. Bolzon, B. A. Schrefler and O. C. Zienkiewicz, 'Elastoplastic soil constitutive laws generalized to partially saturated states', *Geotechnique*, **46**(2), 279–289 (1996).
20. C. Jommi and C. Di Prisco, 'Un semplice approcio teorico per la modellazione del comportamento meccanico di terreni granulari parzialmente saturi, *Proc. Conf. on "Il ruolo dei fluidi nei problemi di ingegneria geotecnia"*, CNR (Italian Research Council), Rome, Vol. 1, 1994, pp. 167–188.
21. A. L. Oeberg and G. Saellfors, 'A rational approach to the determination of the shear strength parameters of unsaturated soils', in *Unsaturated Soils/Sols Non Saturés*, E. E. Alonso and P. Delage (eds), Balkema, Rotterdam, 1995, pp. 151–158.
22. O. Coussy, *Mechanics of Porous Continua*, Wiley and Sons, Chichester, 1995.
23. G. Gudehus, 'Heuristic homogenization of grandulate-liquid aggregates', *Proc. Int. Workshop on Homogenization, Theory of Migration and Granular Bodies*, Technical University of Gdansk, 1995, pp. 103–123.
24. R. S. Sandhu and E. L. Wilson, 'Finite element analysis of flow in saturated porous media', *J. Eng. Mech. Div. ASCE*, **95**, EM3 (1969).
25. J. Ghaboussi and E. L. Wilson, 'Flow of compressible fluid in porous elastic media', *Int. J. numer. methods eng.*, **5**, 419–442 (1973).
26. O. C. Zienkiewicz, A. H. C. Chan, M. Pastor, D. K. Paul and T. Shiomi, 'Static and dynamic behaviour of soils: a rational approach to a quantitative solutions: I. Fully saturated problems', *Proc. R. Soc. London*, **A429**, 285–309 (1990).
27. O. C. Zienkiewicz, Y. M. Xie, B. A. Schrefler, A. Ledesma and N. Bicanic, 'Static and dynamic behaviour of soils: a rational approach to quantitative solutions, II. semi-saturated problems', *Proc. R. Soc. London*, **A429**, 311–321 (1990).

28. E. A. Meroi, B. A. Schrefler and O. C. Zienkiewicz, 'Large strain static and dynamic semisaturated soil behaviour', *Int. j. numer. anal. methods geom.*, **19**, 81–106 (1995).
29. D. Gawin, P. Baggio and B. A. Schrefler, 'Coupled heat, water and gas flow in deformable porous media', *Int. j. numer. methods fluids*, **20**, 969–987 (1995).
30. A. W. Bishop and G. E. Blight, 'Some aspects of effective stress in saturated and partly saturated soils', *Géotechnique*, **13**, 177–197 (1963).
31. B. A. Schrefler and Zhan Xiaoyong, 'A fully coupled model for water flow and airflow in deformable porous media', *Water Resour. Res.*, **29**, 155–167 (1993).
32. A. C. Liakopoulos, 'Transient flow through unsaturated porous media', *Ph.D. Thesis*, Univ. of California, Berkeley, 1965.
33. N. M. Safai and G. F. Pinder, 'Vertical and horizontal land deformation in a desaturating porous medium', *Adv. Water Resources*, **2**, 19–25 (1979).
34. R. N. Brooks and A. T. Corey, 'Properties of porous media affecting fluid flow', *J. Irrig. Drain. Div. Am. Soc. Civ. Eng.*, **92** (IR2), 61–68 (1966).
35. J. Bear and Y. Bachmat, *Introduction to Modeling of Transport Phenomena in Porous Media*, Kluwer, Dordrecht, 1990.
36. D. Gawin and B. A. Schrefler, 'Thermo- hydro- mechanical analysis of partially saturated porous media', *Int. J. Comput. Eng.*, in print.
37. B. A. Schrefler, 'F.E. in environmental engineering: coupled thermo-hydro-mechanical processes in porous media including pollutant transport', *Arch. Comput. Methods Eng. – State of the Art Rev.* **2**, 1–54 (1995).
38. ASHRAE Handbook, *Fundamentals Volume*, ASHRAE, Atlanta, 1993.
39. O. C. Zienkiewicz and R. L. Taylor, *The Finite Element Method*, Vol. 1, 4th edn McGraw Hill, London, 1989.
40. O. C. Zienkiewicz and R. L. Taylor, *The Finite Element Method*, Vol. 2, 4th edn McGraw Hill, London, 1991.
41. T. N. Narasimhan and P. A. Witherspoon, 'Numerical model for saturated-unsaturated flow in deformable porous media. 3. Applications', *Water Resour. Res.*, **14**, 1017–1034 (1978).
42. B. A. Schrefler and L. Simon, 'A unified approach to the analysis of saturated-unsaturated elastoplastic porous media', in G. Svoboda (ed.) *Numerical Methods in Geomechanics*, A. A. Balkema, Rotterdam. 1988, pp. 205–212.
43. O. Krischer and K. Kroell, *Trocknungstechnik, Band. I*, *3.Aufl. Die wissenschaftlichen Grundlagen der Trocknungstechnik*, Springer Verlag, Berlin, 1978.